



Multifrequency geoacoustic imaging of fluid escape structures offshore Costa Rica: Implications for the quantification of seep processes

Ingo Klaucke

*Leibniz Institute of Marine Sciences, IFM-GEOMAR, Wischhofstrasse 1-3, D-24148 Kiel, Germany
(iklaucke@ifm-geomar.de)*

Douglas G. Masson

National Oceanography Centre, Southampton, University of Southampton, Waterfront Campus, European Way, Southampton SO14 3ZH, UK

C. Jörg Petersen

Leibniz Institute of Marine Sciences, IFM-GEOMAR, Kiel, Germany

Now at Department of Geology, University of Tromsø, Drammsveien 201, N-9037 Tromsø, Norway

Wilhelm Weinrebe

Leibniz Institute of Marine Sciences, IFM-GEOMAR, Wischhofstrasse 1-3, D-24148 Kiel, Germany

César R. Ranero

Leibniz Institute of Marine Sciences, IFM-GEOMAR, Kiel, Germany

Now at ICREA, Instituto de Ciencias del Mar, CSIC, Pg. Maritim de la Barceloneta 37-49, E-08003 Barcelona, Spain

[1] Quantification of fluid fluxes from cold seeps depends on accurate estimates of the spatial validity of flux measurements. These estimates are strongly influenced by the choice of geoacoustic mapping tools. Multibeam bathymetry, side-scan sonar, and Chirp subbottom profiler data of several mound-shaped cold seeps offshore central Costa Rica show great variety in morphology and structure although the features are only a few kilometers apart. Mound 11 (a 35 m high and 1000 m in diameter structure), situated in the SE of the study area, has an irregular morphology but a smooth surface on side-scan sonar data, while mound 12 (30 m high, 600 m across) is a cone of more regular outline but with a rough surface, and mound Grillo (5 m high, 500 m across) shows the same rough surface as mound 12 but without relief. Video observations and sediment cores indicate that the structures are formed by the precipitation of authigenic carbonates and indications for extensive mud extrusion are absent, except for one possible mudflow at mound 11. Different sonar frequencies result in variable estimates of the extent of these mounds with low frequencies suggesting much wider cold seeps, consequently overestimating fluid fluxes. The absence of mud volcanism compared to accretionary prisms where mud volcanism occurs is related to different tectonic styles: strong sediment overpressure and thrust faulting in typical accretionary prisms can generate mud volcanism, while subduction erosion and normal faulting (extension) of the overriding plate at the Costa Rican margin result in fluid venting driven by only slight fluid overpressures.



Components: 6947 words, 10 figures, 1 table.

Keywords: cold seeps; Costa Rica; side-scan sonar.

Index Terms: 3045 Marine Geology and Geophysics: Seafloor morphology, geology, and geophysics; 3060 Marine Geology and Geophysics: Subduction zone processes (1031, 3613, 8170, 8413); 3004 Marine Geology and Geophysics: Gas and hydrate systems.

Received 4 June 2007; **Revised** 14 December 2007; **Accepted** 10 January 2008; **Published** 4 April 2008.

Klaucke, I., D. G. Masson, C. J. Petersen, W. Weinrebe, and C. R. Ranero (2008), Multifrequency geoacoustic imaging of fluid escape structures offshore Costa Rica: Implications for the quantification of seep processes, *Geochem. Geophys. Geosyst.*, 9, Q04010, doi:10.1029/2007GC001708.

1. Introduction

[2] Fluids at continental margins play an important role in a number of geological processes. They are believed to lubricate fault planes and the decollement of subduction zones [Segall and Rice, 1995], they may accumulate and form exploitable reservoirs of hydrocarbons [Kvenvolden, 1999], and they are likely to influence the stability of submarine slopes [Sultan *et al.*, 2004]. The expulsion or seepage of fluids at continental margins frequently leads to the precipitation of authigenic carbonates that modify sedimentary processes along the margin, and finally, the fluids constitute the energy source for a number of diverse and complex ecosystems [Sahling *et al.*, 2002]. In order to estimate and quantify the impact of fluid seepage on local ecosystems [Linke *et al.*, 2005] and methane budgets [Mau *et al.*, 2006] a number of model calculations have recently been proposed [Dickens, 2003; Luff and Wallmann, 2003]. These models require knowledge of fluxes and extrapolation of these fluxes regionally or even globally. Measuring fluxes is a problem on its own, but the extrapolation of such estimates must rely on geoacoustic mapping in order to determine the abundance of seeps, and thus the spatial validity of the flux measurements.

[3] Our analysis of different geoacoustic data sets from a small area offshore Costa Rica shows that the choice of mapping tools strongly influences estimates of the extent of fluid seeps. These data sets include multibeam bathymetry and a range of side-scan sonar data, but only very high-resolution side-scan sonar data allow determining the processes that are active at the seep site. Such high-resolution data consequently give insight into the fluid flow system at the erosional Costa Rican margin and indicate that fluid-escape features off-

shore Costa Rica are significantly different from cold seeps at accretionary convergent margins. These differences include the absence of mud volcanism and a high degree of authigenic mineral precipitation and so relate to fluid chemistry, the degree of seep activity and the processes of fluid escape. All these differences will be documented in the present paper and can be attributed to the tectonic style related to subduction erosion processes at the Costa Rican margin. This shows that extrapolation of flux measurements from individual seeps to regional or global models is only likely to be valid if it is based on detailed mapping and includes knowledge of the tectonic environment.

2. Fluid Seepage at Continental Margins

[4] The expulsion of liquids, gases and fluid sediment at continental margins covers a wide range of processes including not only mud volcanism, mud diapirism and gas flares, but also continuously seeping methane-rich fluids leading to cold vent sites and even catastrophic outbursts of overpressured gases [Hovland *et al.*, 2005]. Submarine mud volcanoes in particular have attracted much attention since their discovery some 20 years ago [Langseth *et al.*, 1988]. Due to the increasing availability of multibeam bathymetry data, more and more mud volcanoes or similar positive morphological features have been discovered [Milkov, 2000; Kopf, 2003]. Mud volcanoes appear to be most prominent in areas experiencing compressional tectonics and in passive margin settings with very high sedimentation rates [Kopf, 2003]. More recently, active gas seepage, long recognized in shallow marine settings, has also been discovered in deep water, where it is frequently associated with near-surface deposits of gas hydrates [MacDonald

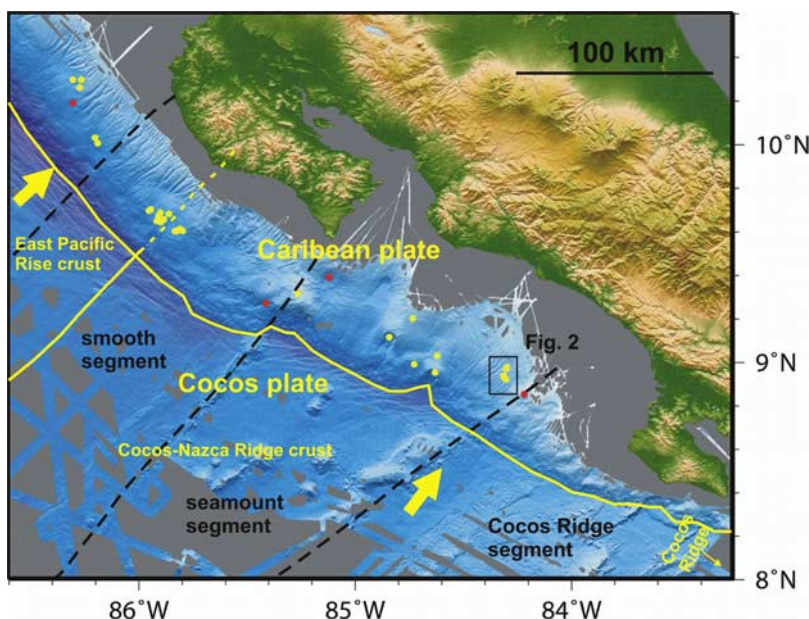


Figure 1. The continental margin offshore Costa Rica showing the different tectonic segments (in black, after *von Huene et al.* [2000]) of the oceanic plates (in yellow) and the distribution of fluid-venting-related structures (from *Sahling et al.*, submitted manuscript, 2008). Dashed lines indicate projected boundaries below the overriding Caribbean Plate. Yellow and red dots indicate mound-like and fault- or slump-related fluid-venting structures, respectively. The arrows indicate the direction of plate movements and subduction.

et al., 2002; *Heeschen et al.*, 2003; *Damm and Budens*, 2003; *Sassen et al.*, 2004; *Klaucke et al.*, 2006]. Many of these fluid seepage sites have only limited relief, often below the detection limit of standard multibeam bathymetry data. Such sites, lacking clear evidence for mud expulsion, will in this paper be referred to geomorphologically as “mounds,” regardless of their actual relief height. Flux measurements are available for only a few of these cold seep sites and display variance of several orders of magnitude between different sites and even within a particular seep location [*Torres et al.*, 2002; *Hensen et al.*, 2004; *de Beer et al.*, 2006].

3. Costa Rica Continental Margin

[5] The morphology and structure of the continental margin offshore Central America is controlled by the subduction of the Cocos Plate beneath the Caribbean Plate (Figure 1). Offshore Costa Rica, the oceanic plates have four different morphotectonic segments [*von Huene et al.*, 2000]. These are from northwest to southeast: rough oceanic crust generated at the East Pacific Rise, smooth oceanic crust generated at the Cocos-Nazca spreading centre, a segment containing many seamounts (the study area is part of this segment), and finally the hot oceanic crust of the Cocos Ridge (Figure 1).

Subduction of all these segments results in tectonic erosion of the overriding plate leading to extension and the formation of large-scale normal faults within this plate [*Ranero and von Huene*, 2000; *von Huene et al.*, 2004; *Hensen et al.*, 2004] and strong subsidence of the entire margin [*Ranero et al.*, 2000; *Vannucchi et al.*, 2003]. In addition, the subduction of seamounts probably accelerates subduction erosion and creates large landslides in the wake of the subducting seamount [*von Huene et al.*, 2000]. All these processes provide pathways for fluid circulation at the Costa Rica margin and a great number of potential fluid-escape features have been identified all along the continental slope [*Bohrmann et al.*, 2002; *H. Sahling et al.*, Fluid seepage at the continental margin off Costa Rica and Nicaragua, submitted to *Geochemistry, Geophysics, Geosystems*, 2008]. The fluid-escape features are concentrated along the mid-slope region of the overriding plate. Several of these fluid-escape features, and in particular those which are the focus of this paper, have been sampled and show indications for active emission of methane-rich fluids [*Hensen et al.*, 2004; *Linke et al.*, 2005; *Mau et al.*, 2006] and even the presence of gas hydrates [*Schmidt et al.*, 2005]. Geochemical analyses of the fluids point toward clay mineral dehydration at the plate boundary as a likely source of the fluids



Table 1. Characteristics of Geoacoustic Data Sets Used for This Study

	EM120 Bathymetry	EM120 Side-Scan	TOBI	DTS1-75	DTS1-410	DTS1-Chirp
Frequency, kHz	11.25/12.6	11.25/12.6	30/32	75	410	2–8
Resolution, m	10	10	6	1	0.25	15 cm ^{a,b}
Penetration ^a		Several meters	<2 m	<1 m	Few cm	Up to 30 m

^a Estimated.

^b Interpretable vertical resolution.

[Hensen *et al.*, 2004], which would then have crossed the entire upper plate before emission at the seafloor. Attempts to quantify methane emissions from measurements of methane concentration in the water column [Mau *et al.*, 2006] show strong variability between different vent sites but suggest that methane emissions at erosive continental margins are less vigorous than methane emissions at accretionary or passive margins.

4. Geoacoustic Data Sets

[6] The data sets used for this study are full ocean depth multibeam bathymetry data including backscatter and pseudo-side-scan information, mid-range side-scan sonar, high-resolution side-scan sonar and high-resolution subbottom profiles (Table 1).

[7] Multibeam bathymetry data were obtained using the Simrad EM120 on board FS SONNE during several cruises. The EM120 system operates at 11.25 and 12.6 kHz and provides 191 beams

with a beam angle of $2 \times 2^\circ$. For each beam both travel time and backscatter amplitude are registered. Finally, the EM120 system also provides a pseudo-side-scan facility based on continuous recording of backscatter signals. Multiple oversampling of the study area due to closely spaced tracks and reduced beam angle allowed processing of the EM120 data to a grid size of 10 m (Figure 2).

[8] Mid-range side-scan sonar data were acquired with the Towed Ocean-Bottom Instrument (TOBI) operated by the National Oceanography Centre, Southampton. TOBI uses 30/32 kHz side-scan sonar with a swath width of just under 6 km and concurrent 6–10 kHz Chirp subbottom profiler. During the FS SONNE cruise SO163-I TOBI was towed about 350 m above the seabed at a speed ranging between 2 and 2.5 knots. Given the horizontal beamwidth of 0.8° for the side-scan sonar, this speed generates a footprint varying from 8×4 m in the near range (500 m) to 40×2 m in the distal range (3000 m). TOBI data were pro-

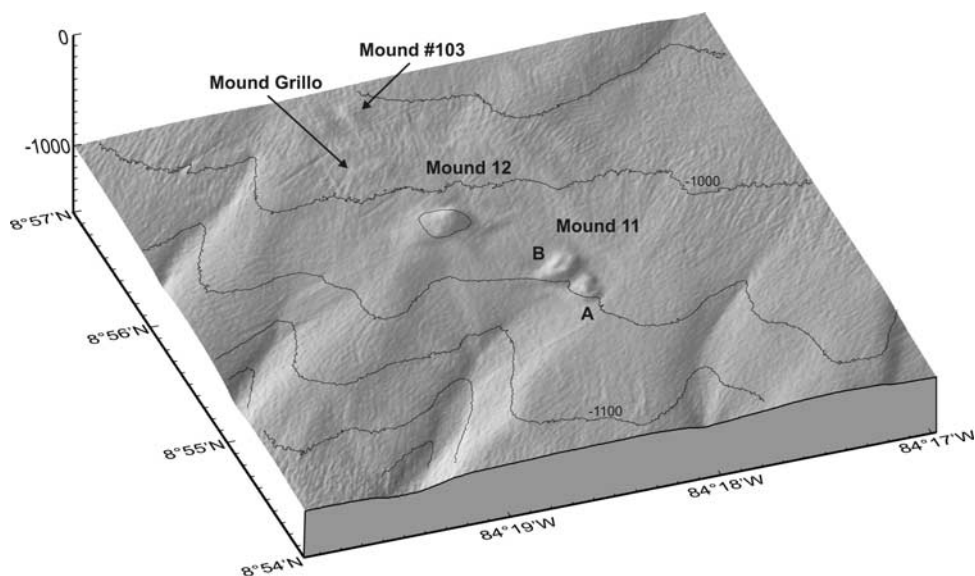


Figure 2. Shaded relief map of the study area offshore Costa Rica showing the two summits of mound 11 as well as mound 12 farther to the northwest. Note that mound Grillo and mound #103 are not resolved by this type of data.

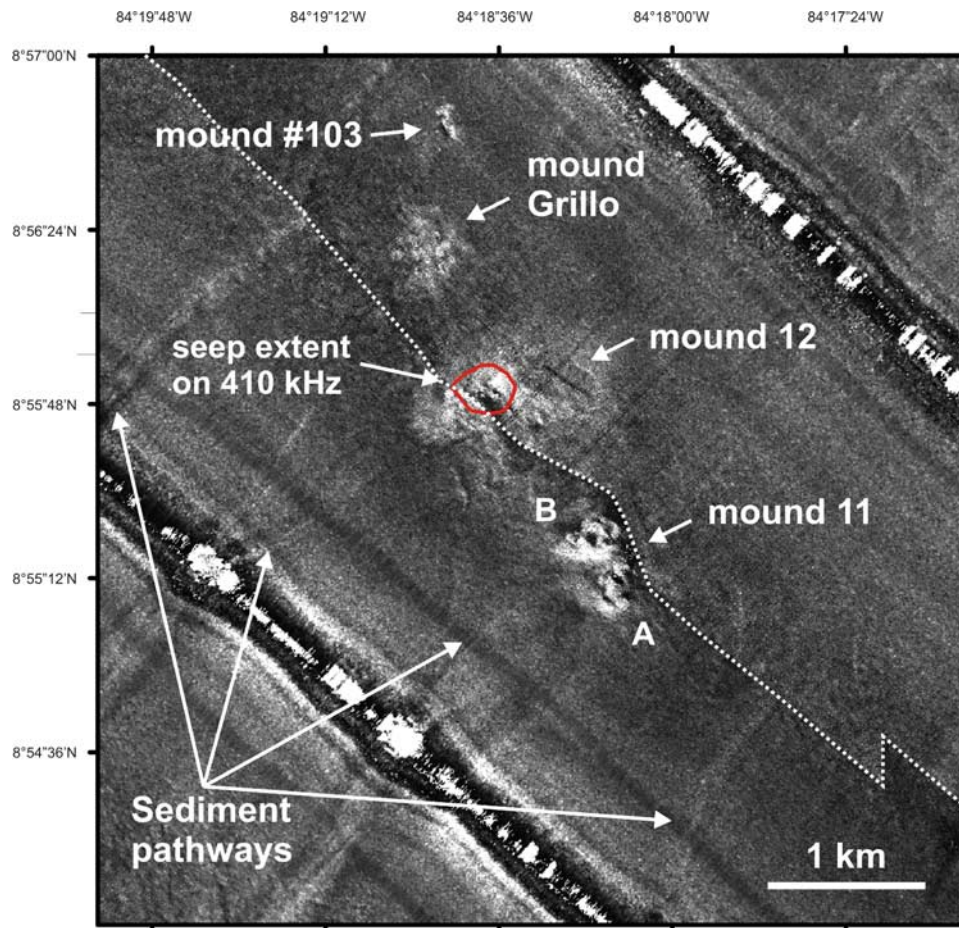


Figure 3. TOBI 30 kHz side-scan sonar mosaic of the study area. High backscatter is shown in light tones. The dashed white line shows the limit of two sonar tracks.

cessed with a pixel size of 6 m using the PRISM package [Le Bas *et al.*, 1995].

[9] High-resolution side-scan sonar data were obtained using the DTS-1 system operated by IFM-GEOMAR during FS SONNE cruise SO173-1. The DTS-1 is a modified EdgeTech dual-frequency Chirp system working with frequencies centered on 75 and 410 kHz giving a maximum range of 750 and 150 m, respectively. The 75 kHz signal is a 14 ms long pulse of 7.5 kHz bandwidth giving an across-track resolution of 5.6 cm. The 410 kHz signal has a bandwidth of 40 kHz and 2.4 ms duration for an across-track-resolution of 1.8 cm. Towing speed averaged 2.5 knots and the data have been processed for a pixel size of 1.0 and 0.25 m respectively, using PRISM. The DTS-1 also includes a Chirp subbottom profiler operating with a 2–8 kHz pulse of 20 ms duration providing up to 40 m of subbottom penetration and a vertical resolution of a few

decimeters. Navigation of the DTS-1 towfish used an ultra-short baseline system providing a nominal precision of 10–20 m, although empirical errors based on mismatch between adjacent survey lines are in the order of 30–40 m.

[10] Side-scan sonar systems operating at different frequencies not only give different horizontal resolution, but also give variable degrees of subbottom signal penetration and volume backscatter [Mitchell, 1993]. Comparison between the side-scan sonar images from the different systems used in this study and information from the 2–8 kHz subbottom profiler indicate that the 75 kHz side-scan sonar signal penetrates less than 2 m, while the 30 kHz side-scan sonar signal appears to register features that are buried by almost 5 m of sediment.

[11] Interpretation of the geoacoustic data sets largely depends on video observations, in situ biogeochemical measurements and sediment cores

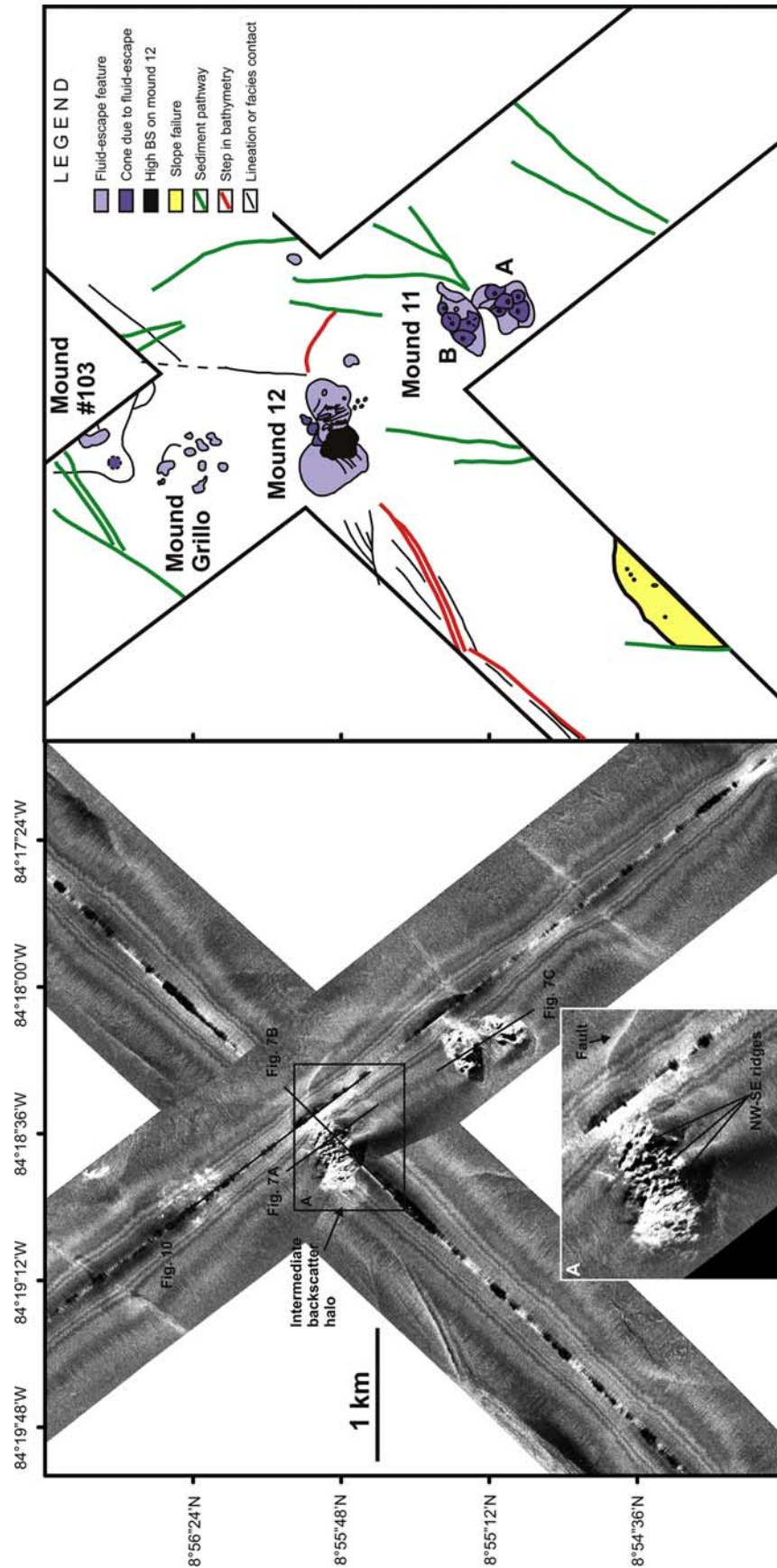


Figure 4. DTS-1 75 kHz side-scan sonar image and interpretation of the study area. High backscatter is shown in light tones.

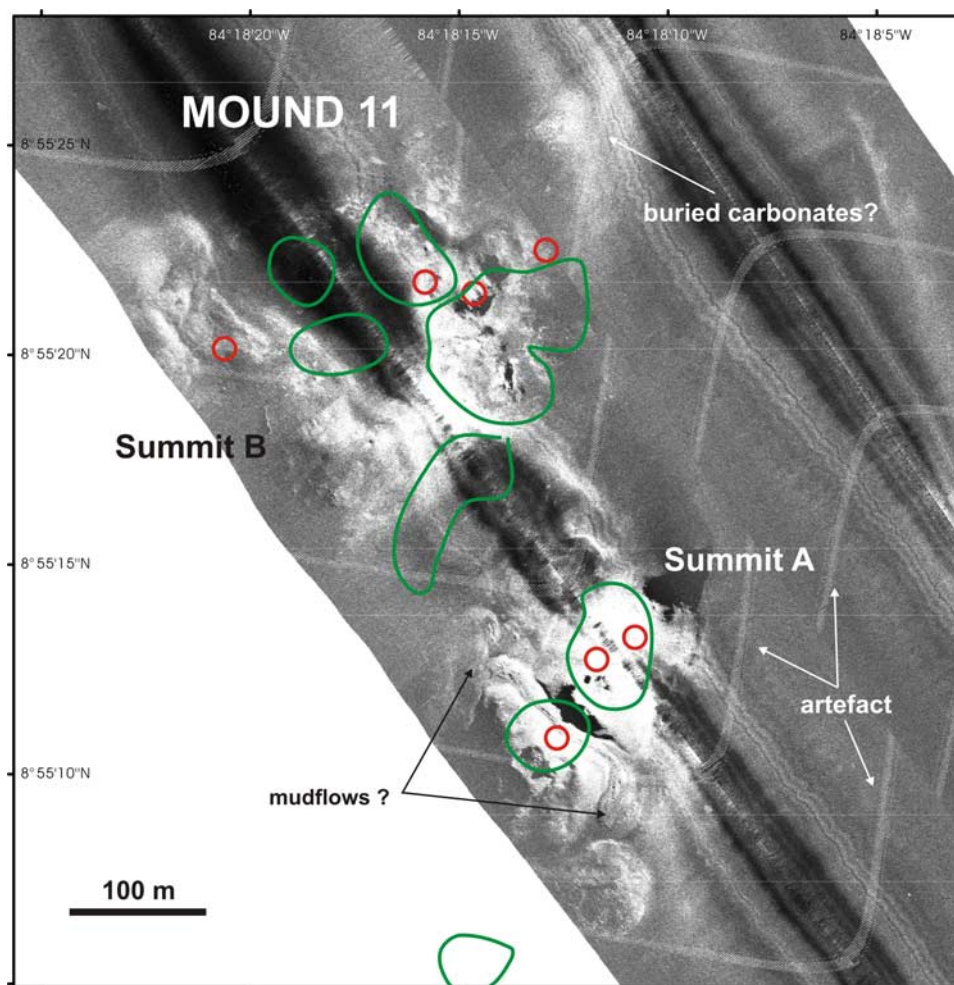


Figure 5. DTS-1 410 kHz side-scan sonar image of mound 11 showing possible small mud extrusion at summit A. The interpretation of towed video profiles of *Mau et al.* [2006], showing the occurrences of bacterial mats (red circles) and carbonates (green outlines), is superimposed. Positioning accuracy of both the side-scan sonar and video data is estimated at ± 25 m.

that have been described previously [*Mörz et al.*, 2005; *Linke et al.*, 2005; *Schmidt et al.*, 2005; *Mau et al.*, 2006].

5. Characteristics of Fluid-Escape Structures

[12] Offshore Costa Rica and Nicaragua a great number of cold seeps related to different structures including landslides, seamount subduction scars, mounds, backscatter anomalies and faults have been identified (*Sahling et al.*, submitted manuscript, 2008). Four of the smaller, mound-shaped cold seeps aligned along a NW-SE direction are the focus of this study (Figure 3). From southeast to northwest these are mound 11 [*Linke et al.*, 2005], mound 12 [*Schmidt et al.*, 2005], a seep structure

without relief named mound Grillo and a small, crest-shaped mound corresponding to seep #103 of *Sahling et al.* (submitted manuscript, 2008).

5.1. Mound 11

[13] Mound 11 is the southeasternmost of the four cold seep structures in the study area. It has two distinct summits (A and B, Figure 2) reaching up to 25 m above the surrounding seafloor. The two summits are 300 m apart and a small slope gully appears to cross the slope between them. Each of the summits is composed of several individual edifices, each up to 250 m in diameter (Figure 4). The surface of these edifices, as of mound 11 in general, is remarkably smooth. This smoothness is particularly well imaged by 410 kHz side-scan sonar data (Figure 5) and contrasts strongly with

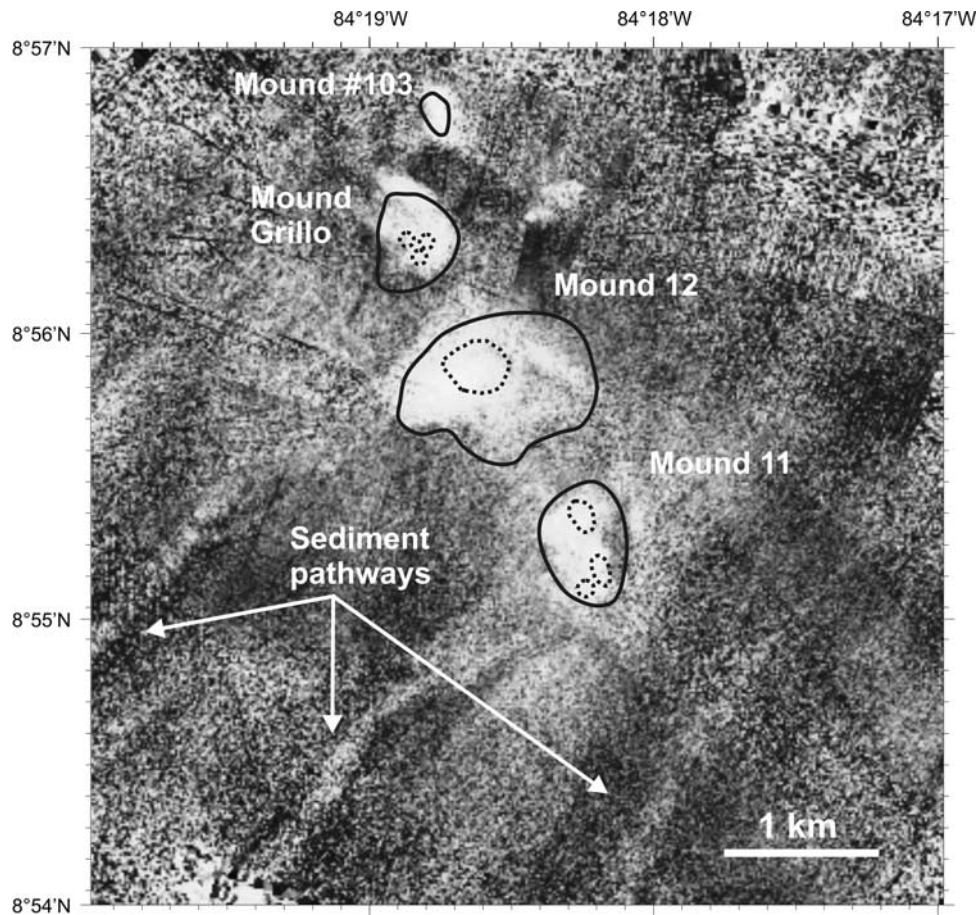


Figure 6. EM120 backscatter image showing the variable extent of high backscatter (white) beyond the positive relief of fluid-escape structures. Solid black lines are the outline of mounds on 30 kHz TOBI side-scan images, and dashed lines are the outline of high backscatter intensity on 410 kHz side-scan images.

the other fluid-escape features in the area. There are no indications for “outliers,” which means that all fluid-seepage activity is concentrated within the double summit area; even backscatter data from the multibeam system does not suggest a wider affected area at depth (Figure 6). Smoothness of the seafloor at mound 11 is probably the effect of sediment cover, as most of the surface of mound 11 is covered by at least 2 m of fine-grained sediments as shown by several gravity cores and by video observation [Schmidt *et al.*, 2005]. The sediment cover does not necessarily imply low fluid-flow activity as video observation of mound 11 showed the presence of bacterial mats at both summits [Hensen *et al.*, 2004; Mau *et al.*, 2006]. Bacterial mats are indicative of elevated methane fluxes and the possible occurrence of gas hydrates at depth [Schmidt *et al.*, 2005].

[14] Two tongue-shaped zones of intermediate backscatter intensity are apparent on either side

of summit A of mound 11 (Figure 5). Each of the two lobes covers about 1500 m². These features could be mud extrusions, but mud extrusions are not known elsewhere on the entire continental slope offshore Costa Rica and Nicaragua. In the absence of “ground-truthing” the feature could also be interpreted as sediment-draped carbonates or small debris flows coming from the steep mound flanks.

5.2. Mound 12

[15] Mound 12 shows a character different from that of mound 11, although the two mounds are only slightly more than 1 km apart. Lower-resolution side-scan sonar images (Figures 3 and 6) indicate a much wider extension of mound 12 at depth than at the seabed, although even at depth it is still well separated from mound 11. Mound 12 consists of only one cone-shaped summit with 30 m relief. Geoacoustically, mound 12 shows a three-

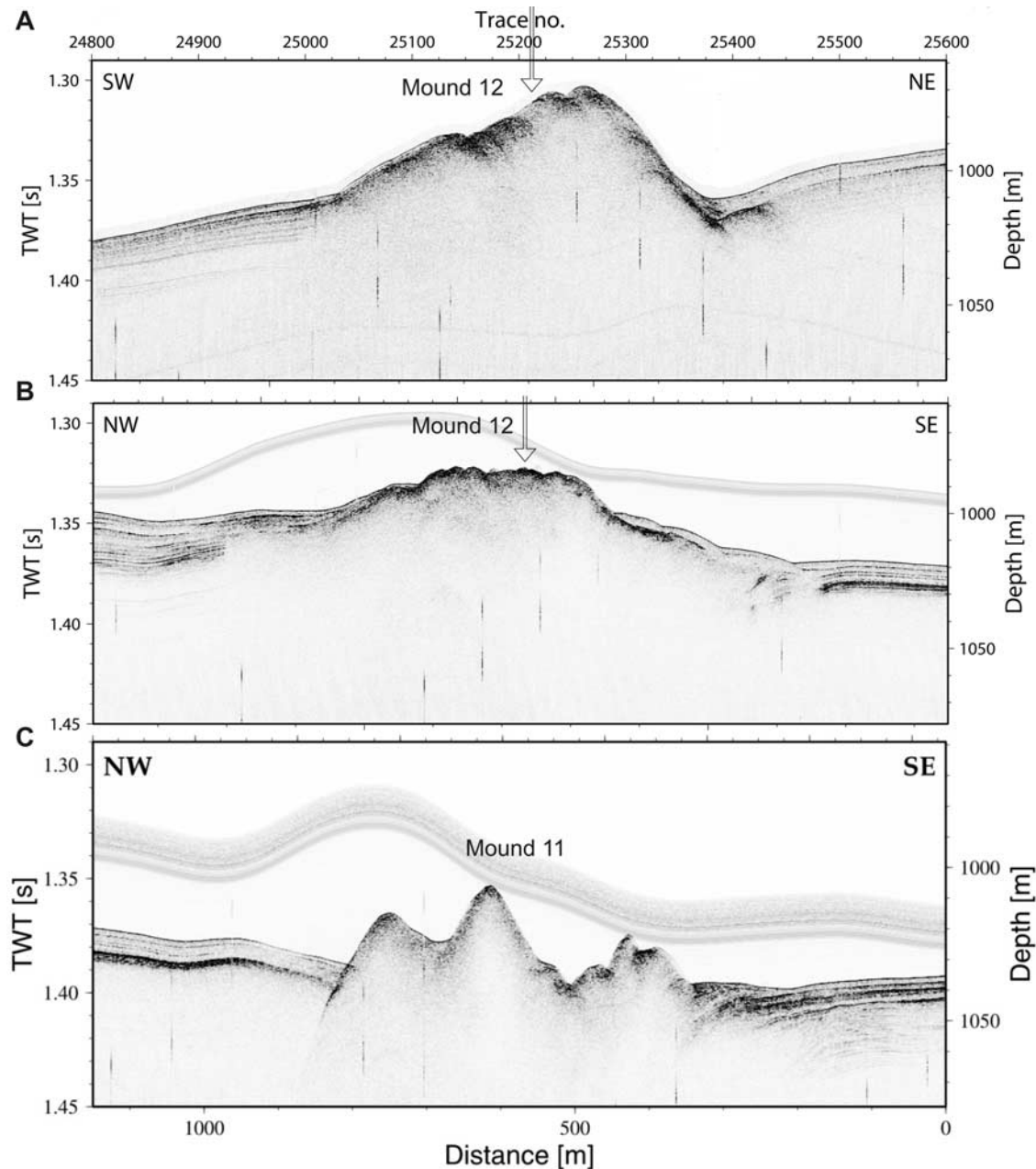


Figure 7. The 2–8 kHz Chirp subbottom profiles crossing fluid-escape features offshore Costa Rica. For profile location, refer to Figure 4. Arrows indicate where profiles crossing mound 12 intersect. Note the presence of the transparent units on the flanks of mound 12.

fold organization, especially on 75 kHz side-scan sonar data (Figure 4). The southern and northern flanks of the mound show backscatter intensities similar to the surrounding sediment, while the summit and the western flank show high backscatter intensity. Subbottom profiler data (Figures 7a and 7b) show that the typical mound facies of the central mound area is covered by a few meters of sediment on the northern and southern flanks, but only very thinly on the western flank. This western

flank is characterized by a 0.05 km² zone of very high backscatter intensity with little internal variation. The high backscatter area is bounded by a small, 100–150 m wide halo of moderate backscatter intensity. The central area of mound 12, on the other hand, shows alternating bands of high backscatter intensity and shadows. These bands are oriented along a NW-SE trend. Very high resolution side-scan sonar images of this area delimit individual, irregular patches, each a few tens of

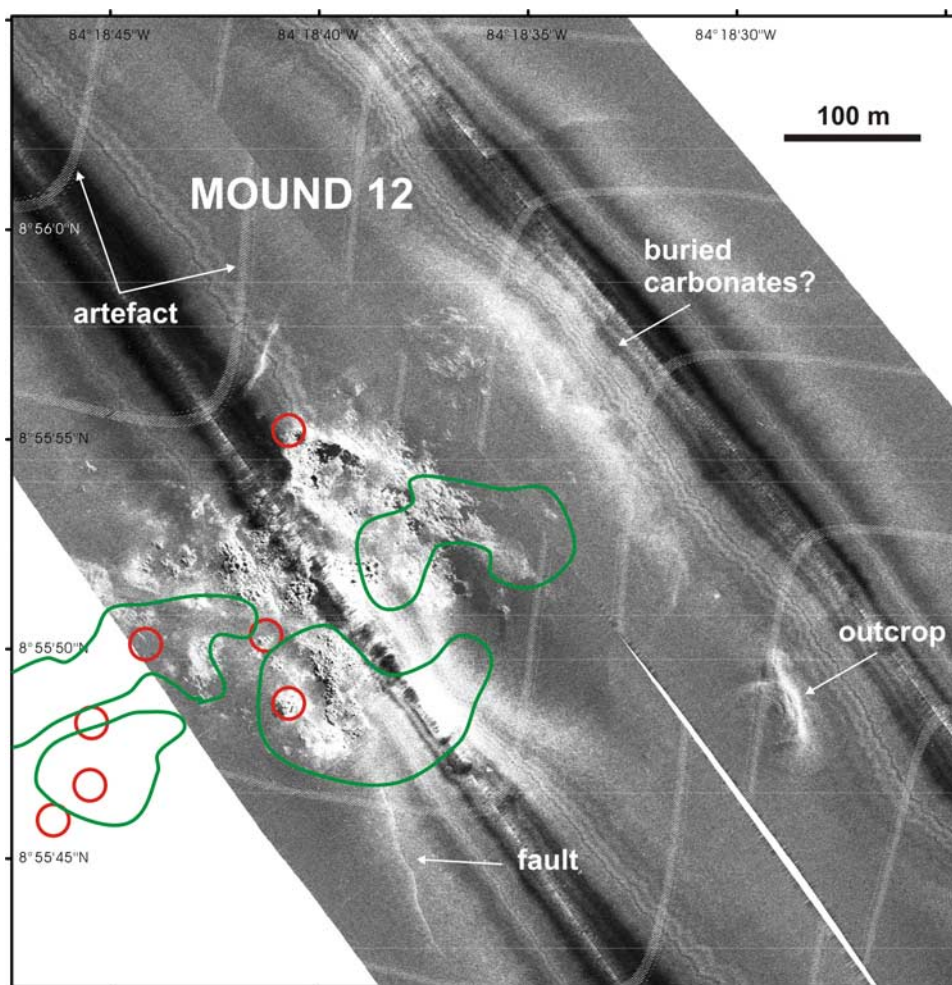


Figure 8. DTS-1 410 kHz side-scan sonar image of mound 12. The interpretation of towed video profiles of *Mau et al.* [2006], showing the occurrences of bacterial mats (red circles) and carbonates (green outlines), is superimposed. Positioning accuracy of both the side-scan sonar and video data is estimated at ± 25 m.

meters in diameter, that appear to have a small positive relief. Video observation [*Linke et al.*, 2005; *Mau et al.*, 2006] suggests that these correspond to carbonate precipitates at the seafloor (Figure 8). A few patches of very high backscatter intensity without relief also exist. Organization of these patches along the NW-SE trending bands shown on 75 kHz side-scan sonar images is not obvious. However, one alignment of high backscatter intensity and similar NW-SE orientation is visible and interpreted as a superficial fault (Figure 8). This fault connects to an elongate carbonate edifice farther north and suggests an underlying fault-control on the distribution of carbonate precipitates. The 75 kHz side-scan image also shows slope-parallel alignments of high backscatter intensity revealing downslope steps in the bathymetry. Whether these steps correspond to fault traces or indicate slope instability cannot be

distinguished beyond doubt with the present data set. The irregular path of the step at the lower margin of the study area (Figure 4), however, points toward a sediment failure.

5.3. Mound Grillo

[16] Another cold seep feature similar to mound 12, although with a relief of less than 5 m, is located about 1 km northwest of the latter. Here, individual patches of high backscatter intensity ranging from less than 10 m to a few tens of meters in diameter are shown on 410 kHz side-scan sonar images (Figure 9). Ground-truth data for these features is not available but by analogy with mound 12 they are interpreted as carbonate precipitates. These patches correlate well with areas of high backscatter intensity on 75 kHz side-scan sonar imagery, but lower-frequency imagery

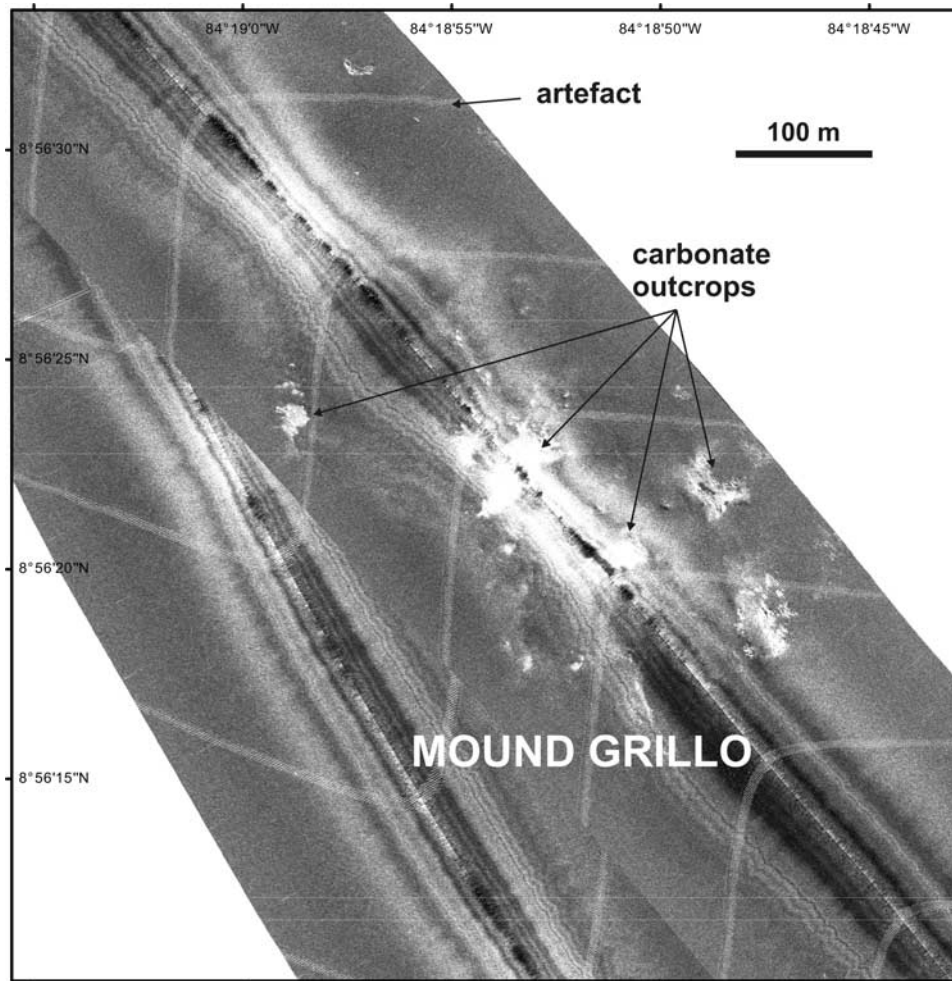


Figure 9. DTS-1 410 kHz side-scan sonar image of the partially buried mound Grillo.

(Figure 3) shows a much larger area of elevated backscatter intensity about 500 m in diameter. This wider extent of the cold seep at depth is confirmed by 2–8 kHz subbottom profiles that image a 5 m

thick layer of acoustically almost transparent deposits outside of the central seep area, overlying a strong reflection interpreted as the top of seep-related carbonates (Figure 10). However, subbot-

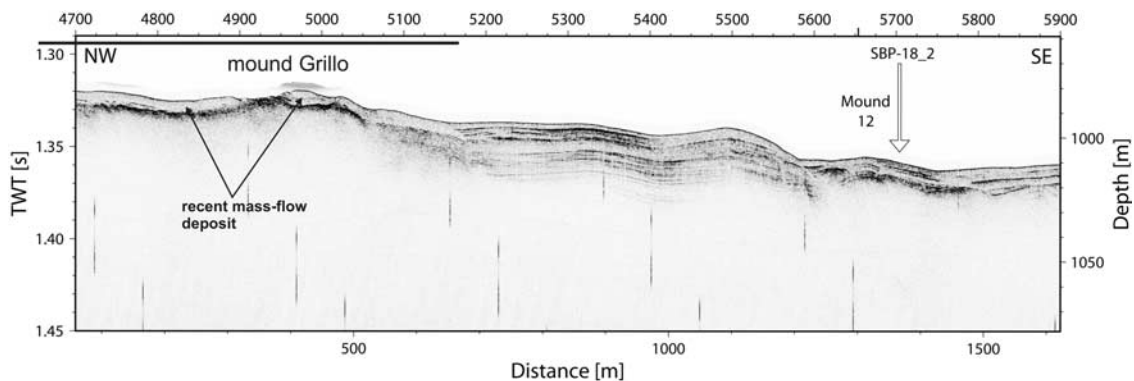


Figure 10. The 2–8 kHz Chirp subbottom profile crossing mound Grillo and the mound 12 area. Note the transparent deposits surrounding mound Grillo compared to crossings of mound 11 and mound 12 (Figure 7). Profile location is indicated on Figure 4.



tom penetration of up to 5 m for the 30 kHz TOBI side-scan sonar data strongly exceeds previous estimates of 30 kHz side-scan sonar penetration [Mitchell, 1993]. Sonar signal attenuation must consequently be much lower than previously estimated or the surficial sediments surrounding the central seep location generate higher backscatter intensities than the normal background sediments, perhaps due to the presence of gas hydrates, seepage-enhanced carbonate cementation, or burial underneath a recent debris flow deposit. All of the latter processes, however, would also result in higher backscatter intensities on 75 kHz side-scan sonar data. This is not observed and the sediment layer covering the interpreted seep-related carbonates appears homogeneous.

5.4. Mound #103

[17] A fourth fluid-escape feature is located some 800 m north of mound Grillo (Figures 3 and 4). This cold seep is characterized by a 250 m long, irregularly shaped ridge oriented NW-SE. Multi-beam backscatter information indicates a much wider extent of this structure at depth with dimensions similar to those of the other cold seeps in the area (Figure 6).

6. Discussion

[18] Are the significant differences between different cold seeps offshore Costa Rica, as shown by geoacoustic data, the result of different processes leading to their formation? Why are there no mud volcanoes offshore Costa Rica as there are in most accretionary prisms? An attempt to look at a wider picture may provide some answers to these questions.

6.1. Mechanism of Fluid Escape

[19] Since the discovery of fluid-escape features with positive relief offshore Costa Rica [Shipley *et al.*, 1990; McIntosh and Silver, 1996; Bohrmann *et al.*, 2002] these features have been termed mud volcanoes [Shipley *et al.*, 1990; McIntosh and Silver, 1996], mud diapirs [Hensen *et al.*, 2004; Schmidt *et al.*, 2005; Linke *et al.*, 2005; Mörz *et al.*, 2005] or mud extrusions [Mau *et al.*, 2006]. None of these terms appears to be justified in the light of detailed field observation. Mud volcanoes are characterized by mudflows or ponded fluidized mud [Brown, 1990], neither of which has been observed on the continental slope offshore Central America, except for a possible small occurrence at mound 11.

[20] Mud volcanism and mud diapirism depend on the formation of overpressured mud at depth. These overpressures are generally attributed to rapid sedimentation or tectonic loading. Buoyancy then drives movement of the mud, which can entrain fluids or create pathways for fluids through shear zones at the edges of the diapir. Fluids can be incorporated into the mud leading to different expressions of mud extrusion ranging from cone-shaped mud volcanoes to mud pies. Such features have been described from many accretionary prisms or passive margin settings with high sedimentation rates [e.g., Henry *et al.*, 1990; Loncke *et al.*, 2004]. High sedimentation rates are generally assumed to be a pre-requisite for the generation of overpressured mud. Offshore Central America, however, sedimentation rate and slope sediment thickness are low. Thickening of sedimentary units as a result of thrusting, as in accretionary prisms, does not occur in the erosive margin offshore Central America. As a consequence conditions for the formation of mud volcanoes are not met. On the other hand, thrust faults require higher fluid overpressures than normal faults for fluids to flow [Sibson, 1981; Behrmann, 1991]. Normal faulting is active across most of the erosive margin offshore Central America [Ranero and von Huene, 2000; Ranero *et al.*, 2007]. As a result, methane-rich fluids generated at the plate boundary by clay mineral dehydration and/or thermal degradation of organic matter migrate through the overriding plate, along the faults, to seep at the seafloor [Hensen *et al.*, 2004; Ranero *et al.*, 2008]. When these fluids interact with seawater, carbonates and other authigenic minerals will precipitate, a process that is strongly mediated by the anaerobic oxidation of methane [Ritger *et al.*, 1987; Boetius and Suess, 2004]. The style of fluid-escape and the absence of mud volcanism appear to be related to the underlying tectonics of the subduction zone. Accretionary subduction zones generate mud volcanoes in the accretionary prism during rapid shortening, loading and pore water migration. Limited fluid escape farther up the slope may also create mud volcanoes related to out of sequence thrusting and deeper fluid origin. Erosive subduction zones such as the study area offshore Costa Rica, on the other hand, provide different pathways for fluid seepage. Due to pervasive normal faulting, fluids can migrate upward without a requirement for high overpressures, which may be reflected in the predominance of authigenic carbonate precipitation and a lack of mud extrusion. This possibly also explains the concentration of fluid-escape features along the middle slope offshore Costa



Rica. In accretionary prisms, fluid-escape commonly occurs near the deformation front (e.g., in Barbados [Langseth *et al.*, 1988]) where mud volcanoes have been described [Henry *et al.*, 1990]. Mud volcanoes are also common features of the Mediterranean Ridge [Camerlenghi *et al.*, 1992; Huguenot *et al.*, 2004] or the Sorokin Trough in the Black Sea [Ivanov *et al.*, 1996], which are both evolved accretionary prisms. On the other hand, side-scan sonar data from the Cascadia accretionary margin show the widespread distribution of authigenic carbonates but no mud volcanoes [Johnson *et al.*, 2003]. Consequently, the tectonic and hydrological system of the Costa Rican margin [Ranero *et al.*, 2008] probably precludes the formation of mud volcanoes, but the absence of mud volcanoes is not a distinctive criterion for erosive margins.

6.2. Mound Evolution

[21] Although closely spaced, the four seep locations studied have distinctly individual characteristics. In the absence of deeper penetrating seismic data it is not known whether they connect to a common reservoir at depth. The seeps are aligned in a NW-SE direction, which also appears as a preferred orientation at the scale of individual mounds. Carbonate precipitates at mound 12 are aligned in this direction (Figure 4). This orientation coincides with the general trend of slope-parallel normal faulting along the Costa Rica margin [Hensen *et al.*, 2004; Ranero *et al.*, 2008] that in turn are a consequence of subduction erosion and suggests that normal faults may govern the distribution of seeps in the study area.

[22] Lateral migration of seep activity along a fault might be responsible for the observed trend from the sediment-covered mound 11 to the fresh mound 12 and a nascent, still mostly buried mound Grillo, a trend that is clearly indicated by both morphology and echofacies. Estimates of methane flux emanating from the mounds [Mau *et al.*, 2006] also supports this trend showing higher activity at mound 12 than mound 11, although data for mound Grillo are missing. On the other hand, mound 11 is still active [Hensen *et al.*, 2004; Schmidt *et al.*, 2005] and does not appear to be clogged by carbonate precipitates. Furthermore, lacking detailed observations and flux estimates at mound Grillo, the alternative explanation that mound Grillo is a dying mound rather than a nascent mound cannot be discarded. An alternative explanation for the observed differences in morphology

and echofacies, based on the location of the seeps on the continental slope, also appears plausible. The continental slope around the seeps is dissected by several canyons and small gullies (Figure 2). It appears that mound 11 is located within a small canyon, while mound 12 sits on top of a ridge between canyons and mound Grillo is located within the next canyon, but could be buried under some recent mass flow deposits. In general, the roughness and appearance of the mounds depends on the balance between fluid flow rate and sedimentation rate (with both potentially being variable). Mound Grillo has been submerged under a recent mass-flow deposit (Figure 10), mound 12 experiences normal hemipelagic sedimentation rates and mound 11 has probably seen some recent erosion by sediment flows.

7. Implications for Fluid-Flow Measurements and Modeling

[23] Fluids escaping at the seafloor may influence ocean chemistry, biogeochemical turnover and climatic changes in ways that are not yet quantified. An increasing number of attempts are being made to quantify fluxes of fluids and chemical species at cold seeps. These attempts are ideally based on direct measurements of these fluxes [e.g., Linke *et al.*, 2005] or involve geochemical modeling in order to explain measured geochemical profiles [e.g., Hensen *et al.*, 2004; Haeckel *et al.*, 2004]. However, both profiles and flux measurements are spatially limited, and the general validity of what are essentially point measurements can only be determined through detailed mapping of the vent site. Video control of the sampling site is a prerequisite, but the area to which the measurements can be extrapolated requires mapping with geoaoustic tools. As the present analysis shows, only very high resolution geoaoustic data can provide a resolution that is comparable to video observations. Such high-resolution data are a prerequisite for estimating the validity of point flux measurements in a regional context, and for extrapolation to regional flux values. Low-frequency sonar data probably overestimate the extent of cold seeps as these data also image buried features. Current published flux estimates are generally not based on high-resolution sonar mapping and must be regarded with the necessary caution. In the case of mounds 11 and 12, for which flux estimates exist, Hensen *et al.* [2004], on the basis of pore water data, report a bacterial mat at mound 11 to be the most active site, while Mau *et al.* [2006]



conclude a methane flux of one magnitude higher at mound 12 compared to mound 11. As our high-resolution sonar images show, both mounds show strong spatial facies variations that most likely reflect different degrees of fluid seepage. Whether these facies variations reflect actual seep processes or represent relict features can only be resolved by dating the carbonate precipitates. In any case, simple extrapolation of local geochemical flux measurements to the entire mound will result in a high degree of uncertainty.

8. Conclusions

[24] Multifrequency side-scan sonar imagery provides a good understanding of cold seep structures at the seafloor and in the shallow subsurface. The resolution of very high frequency side-scan sonar is comparable to video mapping but lacks information about “soft” environments such as bacterial mats. Ground-truthing remains essential in the interpretation of the sonar data.

[25] Fluid-escape structures off Costa Rica are mainly composed of authigenic carbonate precipitates and lack extensive mud extrusions. This reflects the control exerted on fluid flow by the tectonic regime of the area, which is dominated by normal faulting due to subduction erosion. Normal faulting dominates tectonics in erosional margins worldwide [Ranero and von Huene, 2000; von Huene and Ranero, 2003; Sage et al., 2006; Ranero et al., 2006]. Margins of this type form about 50% of all convergent margins [von Huene and Scholl, 1991] and thus the conclusions of this study are possibly representative of global trends.

[26] Differences in the reflectivity pattern of closely spaced mound structures is most likely the result of differential burial by mass wasting deposits and continental slope erosion.

[27] Extrapolation of flux measurements at cold seep sites strongly depends on the choice of the geoaoustic sensor that is used for mapping. Only very high resolution (high-frequency) sensors will provide the basis for reasonable regional flux estimates.

Acknowledgments

[28] The data for this study would not be available without the professionalism of masters, officers, crews, and scientists of FS SONNE cruises SO163 and SO173. Funding for the cruises and subsequent work was provided by the German Ministry of Education and Research (BMBF), the German

Research Foundation (DFG), and the United Kingdom Natural Environment Research Council (NERC). This is contribution 79 of the Sonderforschungsbereich 574 “Volatiles and fluids in subduction zones” at Kiel University. Three anonymous reviews pointed out shortcomings of the original submission and helped improve the paper.

References

- Behrmann, J. (1991), Conditions for hydrofracture and the fluid permeability of accretionary prisms, *Earth Planet. Sci. Lett.*, *107*, 550–558.
- Boetius, A., and E. Suess (2004), Hydrate Ridge: A natural laboratory for the study of microbial life fuelled by methane from near-surface gas hydrates, *Chem. Geol.*, *205*, 291–310.
- Bohrmann, G., et al. (2002), Widespread fluid expulsion along the seafloor of Costa Rica convergent margin, *Terra Nova*, *14*, 69–79.
- Brown, K. M. (1990), Nature and hydrogeological significance of mud diapirs and diatremes for accretionary systems, *J. Geophys. Res.*, *95*, 8969–8982.
- Camerlenghi, A., M. B. Cita, W. Hieke, and T. Ricchiuto (1992), Geological evidence for mud diapirism on the Mediterranean Ridge accretionary complex, *Earth Planet. Sci. Lett.*, *109*, 493–504.
- Damm, E., and G. Budens (2003), Fate of vent-derived methane in seawater above Haakon Mosby mud volcano (Norwegian Sea), *Mar. Chem.*, *82*, 1–11.
- de Beer, D., E. Sauter, H. Niemann, N. Kaul, J.-P. Foucher, U. Witte, M. Schlüter, and A. Boetius (2006), In situ fluxes and zonation of microbial activity in surface sediments of the Haakon Mosby Mud Volcano, *Limnol. Oceanogr.*, *51*, 1315–1331.
- Dickens, G. R. (2003), Rethinking the global carbon cycle with a large, dynamic and microbially mediated gas hydrate capacitor, *Earth Planet. Sci. Lett.*, *213*, 169–183.
- Haeckel, M., E. Suess, K. Wallmann, and D. Rickert (2004), Rising methane gas bubbles form massive hydrate layers at the seafloor, *Geochim. Cosmochim. Acta*, *68*, 4335–4345.
- Heeschen, K. U., A. M. Tréhu, R. W. Collier, E. Suess, and G. Rehder (2003), Distribution and height of methane bubble plumes on the Cascadia Margin characterized by acoustic imaging, *Geophys. Res. Lett.*, *30*(12), 1643, doi:10.1029/2003GL016974.
- Henry, P., X. Le Pichon, S. Lallemand, J.-P. Foucher, G. K. Westbrook, and M. Hobart (1990), Mud volcano field seaward of the Barbados Accretionary complex: A deep towed sidescan sonar survey, *J. Geophys. Res.*, *95*, 8917–8929.
- Hensen, C., K. Wallmann, M. Schmidt, C. R. Ranero, and E. Suess (2004), Fluid expulsion related to mud extrusion off Costa Rica—A window to the subducting slab, *Geology*, *32*, 201–204.
- Hovland, M., H. Svensen, C. F. Forsberg, H. Johansen, C. Fichler, J. H. Fosså, R. Jonsson, and H. Rueslåtten (2005), Complex pockmarks with carbonate-ridges off mid-Norway: Products of sediment degassing, *Mar. Geol.*, *218*, 191–206.
- Huguen, C., J. Mascle, E. Chaumillon, R. Gribouard, A. Kopf, and J. Woodside (2004), Structural setting and tectonic control on mud volcanoes: Evidences from the Central and Eastern Mediterranean Ridge from geophysical data, *Mar. Geol.*, *209*, 245–263.
- Ivanov, M. K., A. F. Limonov, and T. C. E. van Weering (1996), Comparative characteristics of the Black Sea and Mediterranean Ridge mud volcanoes, *Mar. Geol.*, *132*, 253–271.



- Johnson, J. E., C. Goldfinger, and E. Suess (2003), Geophysical constraints on the surface distribution of authigenic carbonates across the Hydrate Ridge region, Cascadia margin, *Mar. Geol.*, *202*, 79–120.
- Klaucke, I., H. Sahling, W. Weinrebe, V. Blinova, D. Bürk, N. Lursmanashvili, and G. Bohrmann (2006), Acoustic investigation of cold seeps offshore Georgia, eastern Black Sea, *Mar. Geol.*, *231*, 51–67.
- Kopf, A. (2003), Global methane emission through mud volcanoes and its past and present impact on the Earth's climate, *Int. J. Earth Sci.*, *92*, 806–816.
- Kvenvolden, K. A. (1999), Potential effects of gas hydrate on human welfare, *Proc. Natl. Acad. Sci. U. S. A.*, *96*, 3420–3426.
- Langseth, M., G. K. Westbrook, and M. A. Hobart (1988), Geophysical survey of a submarine mud volcano seaward of the Barbados Ridge Accretionary Complex, *J. Geophys. Res.*, *93*, 1049–1061.
- Le Bas, T. P., D. C. Mason, and N. W. Millard (1995), TOBI image processing—The state of the art, *IEEE J. Oceanic Eng.*, *20*, 85–93.
- Linke, P., K. Wallmann, E. Suess, C. Hensen, and G. Rehder (2005), In-situ benthic fluxes from an intermittently active mud volcano at the Costa Rica convergent margin, *Earth Planet. Sci. Lett.*, *235*, 79–95.
- Loncke, L., J. Mascle, and Fanil Scientific Parties (2004), Mud volcanoes, gas chimneys, pockmarks and mounds in the Nile deep sea fan (eastern Mediterranean): Geophysical evidences, *Mar. Petrol. Geol.*, *21*, 669–689.
- Luff, R., and K. Wallmann (2003), Fluid flow, methane fluxes, carbonate precipitation and biogeochemical turnover in gas hydrate-bearing sediments at Hydrate Ridge, Cascadia Margin: Numerical modelling and mass balances, *Geochim. Cosmochim. Acta*, *67*, 3403–3421.
- MacDonald, I. R., I. Leifer, R. Sassen, P. Stine, R. Mitchell, and N. Guinasso, Jr. (2002), Transfer of hydrocarbons from natural seeps to the water column and atmosphere, *Geofluids*, *2*, 95–107.
- Mau, S., H. Sahling, G. Rehder, E. Suess, P. Linke, and E. Soeding (2006), Estimates of methane output from mud extrusions at the erosive convergent margin off Costa Rica, *Mar. Geol.*, *225*, 129–144.
- McIntosh, K., and E. Silver (1996), Using 3-D seismic reflection data to find seeps from the Costa Rica accretionary prism, *Geophys. Res. Lett.*, *23*, 895–898.
- Milkov, A. V. (2000), Worldwide distribution of submarine mud volcanoes and associated gas hydrates, *Mar. Geol.*, *167*, 29–42.
- Mitchell, N. C. (1993), A model for attenuation of backscatter due to sediment accumulation and its application to determine sediment thickness with GLORIA sidescan sonar, *J. Geophys. Res.*, *98*, 22,477–22,493.
- Mörz, T., et al. (2005), Styles and productivity of mud diapirism along the Middle American Margin: Part II. Mound Culebra and Mounds 11 and 12, in *Mud Volcanoes, Geodynamics and Seismicity, NATO Sci. Ser., Ser. IV*, vol. 51, edited by G. Martinelli and B. Panahi, pp. 49–76, Springer, Dordrecht, Netherlands.
- Ranero, C. R., and R. von Huene (2000), Subduction erosion along the Middle America convergent margin, *Nature*, *404*, 748–752.
- Ranero, C. R., R. von Huene, E. Flueh, M. Duarte, D. Baca, and K. McIntosh (2000), A cross section of the convergent Pacific margin of Nicaragua, *Tectonics*, *19*, 335–357.
- Ranero, C. R., R. von Huene, W. Weinrebe, and C. Reichert (2006), Tectonic processes along the Chile Convergent Margin, in *The Andes: Active Subduction Orogeny*, vol. 1, *Frontiers Earth Sci.*, vol. XXII, edited by O. Oncken, et al., pp. 91–121, Springer, Berlin.
- Ranero, C. R., R. von Huene, W. Weinrebe, and U. Barckhausen (2007), Convergent margin tectonics of Middle America: A marine perspective, in *Central America, Geology, Hazards and Resources*, edited by G. Alvarado and J. Bunsch, pp. 239–265, A. A. Balkema, Brookfield, Vt.
- Ranero, C. R., I. Grevemeyer, H. Sahling, U. Barckhausen, C. Hensen, K. Wallmann, W. Weinrebe, P. Vannucchi, R. von Huene, and K. McIntosh (2008), The hydrogeological system of erosional convergent margins and its influence on tectonics and interplate seismogenesis, *Geochem. Geophys. Geosyst.*, doi:10.1029/2007GC001679, in press.
- Ritger, S., B. Carson, and E. Suess (1987), Methane derived authigenic carbonates formed by subduction-induced pore-water expulsion along the Oregon/Washington margin, *Geol. Soc. Am. Bull.*, *98*, 147–156.
- Sage, F., J. Y. Collot, and C. R. Ranero (2006), Interplate patchiness and subduction-erosion mechanisms: Evidence from depth-migrated seismic images at the central Ecuador convergent margin, *Geology*, *34*, 997–1000, doi:10.1130/G22790A.1.
- Sahling, H., D. Rickert, R. W. Lee, P. Linke, and E. Suess (2002), Macrofaunal community structure and sulfide flux at gas hydrate deposits from the Cascadia convergent margin, NE Pacific, *Mar. Ecol. Prog. Ser.*, *231*, 121–138.
- Schmidt, M., C. Hensen, T. Mörz, C. Müller, I. Grevemeyer, K. Wallmann, S. Mau, and N. Kaul (2005), Methane hydrate accumulation in 'Mound 11' mud volcano, Costa Rica forearc, *Mar. Geol.*, *216*, 83–100.
- Sassen, R., H. H. Roberts, R. Carney, A. V. Milkov, D. A. deFreitas, B. Lanoil, and C. Zhang (2004), Free hydrocarbon gas, gas hydrate, and authigenic minerals in chemosynthetic communities of the northern Gulf of Mexico continental slope: Relation to microbial processes, *Chem. Geol.*, *205*, 195–217.
- Segall, P., and J. R. Rice (1995), Dilatancy, compaction, and slip instability of a fluid saturated fault, *J. Geophys. Res.*, *100*, 22,155–22,171.
- Shibley, T. H., P. L. Stoffa, and D. F. Dean (1990), Underthrust sediments, fluid migration pathways, and mud volcanoes associated with the accretionary wedge off Costa Rica: Middle America Trench, *J. Geophys. Res.*, *95*, 8743–8752.
- Sibson, R. H. (1981), Controls on low-stress hydro-fracture dilatancy in thrust, wrench and normal fault terrains, *Nature*, *289*, 665–667.
- Sultan, N., et al. (2004), Triggering mechanisms of slope instability processes and sediment failures on continental margins: A geotechnical approach, *Mar. Geol.*, *213*, 291–321.
- Torres, M. E., J. McManus, D. E. Hammond, M. A. de Angelis, K. U. Heeschen, S. L. Colbert, M. D. Tryon, K. M. Brown, and E. Suess (2002), Fluid and chemical fluxes in and out of sediments hosting methane hydrate deposits on Hydrate Ridge, OR, I: Hydrological provinces, *Earth Planet. Sci. Lett.*, *201*, 525–540.
- Vannucchi, P., C. R. Ranero, S. Galeotti, S. M. Straub, D. W. Scholl, and K. McDougall-Ried (2003), Fast rates of subduction erosion along the Costa Rica Pacific margin: Implications for nonsteady rates of crustal recycling at subduction zones, *J. Geophys. Res.*, *108*(B11), 2511, doi:10.1029/2002JB002207.
- von Huene, R., and C. R. Ranero (2003), Subduction erosion and basal friction along the sediment-starved convergent margin off Antofagasta, Chile, *J. Geophys. Res.*, *108*(B2), 2079, doi:10.1029/2001JB001569.



von Huene, R., and D. W. Scholl (1991), Observations at convergent margins concerning sediment subduction, subduction erosion, and the growth of continental crust, *Rev. Geophys.*, *29*, 279–316.

von Huene, R., C. R. Ranero, W. Weinrebe, and K. Hinz (2000), Quaternary convergent margin tectonics of Costa

Rica, segmentation of the Cocos Plate, and Central American volcanism, *Tectonics*, *19*, 314–334.

von Huene, R., C. R. Ranero, and P. Vannucchi (2004), Generic model of subduction erosion, *Geology*, *32*, 913–916.